Journal of Applied Pharmaceutical Research
Volume 13 Issue 5, Year of Publication 2025, Page 254 – 270
DOI: https://doi.org/10.69857/joapr.v13i5.1450

Check for updates

Research Article

JOURNAL OF APPLIED PHARMACEUTICAL RESEARCH | JOAPR
www.japtronline.com

PHYTOCHEMICAL PROFILING AND IN SILICO EVALUATION OF BRASSICA OLERACEA STEM BIOACTIVES AS NOVEL ALDOSE REDUCTASE INHIBITORS FOR DIABETIC NEUROPATHY TREATMENT

Rajashree Dadasaheb Ghogare[1]*, Rahul Rajendra Kunkulol[2], Deepak Babasaheb Nehe[3]

Article Information
Received: 10th June 2025
Revised: 5th September 2025
Accepted: 1st October 2025
Published: 31st October 2025

Keywords
Brassica oleracea, aldose reductase inhibitor, diabetic neuropathy, molecular docking, ADME analysis, drug-likeness.

ABSTRACT

Background: Diabetic neuropathy affects over 50% of diabetic patients, causing significant morbidity and economic burden exceeding $327 billion annually. Current treatments offer limited relief, accompanied by considerable side effects. Aldose reductase inhibition represents a promising therapeutic approach, yet synthetic inhibitors face clinical challenges, including hepatotoxicity and inadequate safety margins. This study investigates *Brassica oleracea* stem bioactives as novel aldose reductase inhibitors. **Methodology:** Sequential extraction of *Brassica oleracea* stems employed ethanol and acetone solvents. Phytochemical screening utilized standard chemical tests, while HR-LCMS enabled metabolite identification. Molecular docking against human aldose reductase (PDB: 1US0) was performed using GeinDock Suite. Drug-likeness and ADME properties were assessed using SwissADME, in accordance with Lipinski's Rule of Five. Comprehensive pharmacokinetic parameters were also evaluated. **Results and Discussion:** HR-LCMS identified 33 bioactive compounds with identification scores >90%. Four lead compounds demonstrated optimal aldose reductase inhibitory potential with superior drug-likeness: Indole-3-acetonitrile (-8.9 kcal/mol, Ki=0.30 μM) approached reference inhibitors epalrestat (-9.9 kcal/mol) and sorbinil (-9.4 kcal/mol) with zero Lipinski violations. 18-Oxooleate (-7.5 kcal/mol) and Salicylamide (-7.6 kcal/mol) exhibited exceptional bioavailability (0.85) with minimal CYP450 inhibition. Phytosphingosine (-6.7 kcal/mol) displayed advantageous peripheral selectivity. **Conclusion:** Four *B. oleracea* compounds demonstrate optimal convergence of aldose reductase inhibitory potential and pharmaceutical feasibility, offering promising orally bioavailable candidates for diabetic neuropathy management. Their natural origin and favorable ADME profiles warrant immediate progression to in vitro validation and in vivo studies.

[1]*Pravara Rural College of Pharmacy, Loni, Tal - Rahata, Dist – Ahilyanagar, 413736, India.*
[2]*Pravara Institute of Medical Science, Loni, Tal - Rahata, Dist – Ahilyanagar, 413736, India.*
[3]*Padmashri Vikhe Patil College of Arts science & commerce, Pravaranagar, Tal - Rahata, Dist – Ahilyanagar, 413712, India.*

For Correspondence:** **rajshrighogare9@gmail.com

INTRODUCTION

Diabetic neuropathy is a serious problem for people with diabetes, and it currently affects more than half of all adults who have diabetes [1]. This condition leads to pain, numbness, and eventually muscle weakness, which reduces the quality of life and puts a burden on the healthcare system [2]. Every year, there is a worldwide economic loss of more than $327 billion, and around a third of healthcare costs for diabetes are attributed to diabetic neuropathy [3]. At present, drugs commonly used to treat addiction are anticonvulsants, antidepressants, and opioids, but they provide limited relief and may cause patients to feel sleepy, confused, and dependent [4]. Even with years of studies, treatments that can slow or halt disease progression have not been found, which clearly points to the urgent need for another approach. Recent discoveries have suggested that the polyol pathway, particularly the aldose reductase enzyme, is primarily responsible for diabetic neuropathy; therefore, blocking aldose reductase could be a promising approach to treating it [5].

Aldose reductase, located in the cytoplasm and belonging to the oxidoreductase family, catalyzes the conversion of glucose into sorbitol via the polyol pathway, thereby regulating the entire process [6]. When there is too much sugar in the blood, sorbitol is produced in the cells, leading to excessive water retention, depletion of myoinositol, a less active Na+/K+-ATPase, and problems with nerve function [7]. The enzyme's structure exhibits a TIM-barrel fold and a pocket that is sufficiently deep to accommodate both NADPH and substrate molecules. Some examples of these types of medications, including epalrestat, fidarestat, and ranirestat, have been evaluated in clinical research, indicating modest effectiveness but limited clinical use due to liver toxicity, difficulty achieving adequate blood levels, and inadequate safety margins [8]. The place where the enzyme functions has four crucial amino acid residues, namely Tyr48, Trp20, His110, and Gln183, that play a role in trapping potential inhibitors [9]. Investigations using crystallography have revealed that the active site can assume different shapes, opening up new opportunities for designing drugs that can bind to specific shapes within the binding site [10]. Currently approved pharmaceuticals often rely on natural products for their origin, with plant-based compounds being valued for their diverse structures and biological activities, and are generally considered less risky [11]. The Cruciferae family includes *Brassica oleracea*, commonly known as wild cabbage, which is used globally for its leaves, stems, and inflorescences. Typically seen as a byproduct of agriculture, the stem part contains numerous bioactive substances, including glucosinolates, phenolic compounds, flavonoids, and terpenoids, several of which have proven anti-diabetic effects [12]. According to phytochemical studies, specific metabolites, such as chalcones, ecdysteroids, and glycosylated flavonoids, are predominantly found in the stem portion of the plant [13]. They are known to act as antioxidants, fight inflammation, and regulate enzymes, suggesting that they may have other therapeutic effects beyond being nutrients. Scientists can utilize agri-food waste to develop medications, adhering to the principles of sustainability and obtaining cost-effective materials [14]. The long-standing worldwide use of Brassica species demonstrates that Brassica compounds are safe, potentially allowing them to be used more rapidly in healthcare than artificial chemical agents [15]. The study aims to identify the chemical composition of stem extracts from Brassica oleracea and evaluate their ability to inhibit aldose reductase using computational methods. Among the objectives are identifying and quantifying bioactive metabolites, determining if these metabolites exhibit suitable drug-like properties using computer models, and investigating their interactions with human aldose reductase to establish a connection between their structure and activity.

MATERIALS AND METHODS

Materials

Fresh *Brassica oleracea* stems were collected from local agricultural fields in Maharashtra, India, and authenticated by the Department of Botany and Research, Centre Padmashri Vikhe Patil College of Arts, Science and Commerce, Pravaranagar, 413713 (Ref. No. PVPC/Bot/2021-22/HD-74). Ethanol (analytical grade, 99.5% purity) was procured from Sciquaint Chemicals (Pune, India). Acetone (analytical grade, 99.8% purity) was obtained from Sciquaint Innovations Pvt. Ltd. (Pune, India). Formic acid (LC-MS grade, 98% purity) and acetonitrile (LC-MS grade, 99.9% purity) were sourced from Neeta Chemicals (Pune, India). Ultra-pure water (LC-MS grade) was prepared using a Milli-Q system. Dragendorff's reagent components, including bismuth nitrate and potassium iodide (analytical grade), were purchased from Research Lab Fine Chem Industries (Pune, India). Aluminum chloride (10% solution, analytical grade), ferric chloride (5% solution, analytical grade), α-naphthol reagent, acetic anhydride, and concentrated sulfuric acid (analytical grade) were obtained from Sciquaint Chemicals (Pune, India). Filter papers (Whatman No.

1) and amber-colored storage vials were procured from local laboratory suppliers. All other chemicals & reagents used in this study were of analytical grade and obtained from certified suppliers in Pune, India.

Methods

Collection and Extraction of Materials

During the harvest season (October-November 2023), Fresh *Brassica oleracea* stems were sourced from local farms in Maharashtra, India, and the Department of Botany, University of Pune acknowledged them (voucher specimen no. BO-ST-2023). Distilled water was used to wash the stems, which were then left to dry in the shade at average room temperature (25±2°C) for 15 days. After that, the powder was obtained by grinding the washed, dried stems with a mechanical grinder manufactured by Remi Motors in India. Sequential extraction was performed using a Soxhlet apparatus (Borosil Glass Works Ltd.). Ethanol (99.5% analytical grade, Merck Life Sciences Pvt. Ltd.) and acetone (99.8% analytical grade, SRL Pvt. Ltd.) were used as solvents. A solvent-to-sample ratio of 10:1 (v/w) was used for 8 hours of extraction at 60°C. After filtering through Whatman No. 1 filter paper, concentration was achieved by using a rotary evaporator from IKA India Pvt. Ltd. in Bangalore at 40°C. The dried extracts were placed into amber vials and stored at -20°C before further study [16,17].

Phytochemical Analysis

Chemical tests were used to study and identify the primary groups of secondary metabolites present in the ethanolic and acetone extracts of the stems. Dragendorff's reagent was prepared with bismuth nitrate and potassium iodide purchased from Hi-Media Laboratories Pvt. Ltd., Mumbai, and was successful at detecting alkaloids through orange-red precipitate formation. The aluminum chloride test was performed using 10% $AlCl_3$ (Sisco Research Laboratories, Mumbai, India), and the development of a yellow coloration indicated the presence of flavonoids. After adding the $FeCl_3$ solution, positive detection of phenolic compounds resulted in a change in color to blue-green (Merck Life Sciences Pvt. Ltd., Mumbai, India). Distilled water was used for the foam test to detect saponins, whereas glycosides were tested with Molisch's test (using α-naphthol reagent from SRL Pvt. Ltd., Mumbai, India) and concentrated sulfuric acid. Positive identification of terpenoids was made with Liebermann-Burchard test using acetic anhydride and concentrated sulfuric acid from Hi-Media Laboratories Pvt. Ltd [18,19].

LCMS Analysis

Liquid chromatography-mass spectrometry analysis was conducted on a Waters Acquity UPLC system coupled to a Thermo Fisher Scientific Q-Exactive Orbitrap mass spectrometer to comprehensively characterize the metabolites in the stem extracts. Chromatographic separation was performed on a 2.1×100 mm Acquity UPLC BEH C18 column (1.7 μm particle size, Waters India Pvt. Ltd., Bangalore, India) maintained at 40°C with an injection volume of 5 μL.

The mobile phase consisted of (A) 0.1% formic acid in water and (B) 0.1% formic acid in acetonitrile, delivered at a flow rate of 0.3 mL/min using the following gradient program: 0-1 min, 5% B; 1-10 min, 5-95% B; 10-12 min, 95% B; 12-12.1 min, 95-5% B; 12.1-15 min, 5% B.Mass spectrometric detection was performed in both positive (ESI+) and negative (ESI−) electrospray ionization modes with the following parameters: spray voltage 3.5 kV, capillary temperature 320°C, sheath gas flow 10 arbitrary units, scan range m/z 100-1500, and resolution 70,000 FWHM. Data acquisition was performed using Xcalibur software (version 4.2, Thermo Fisher Scientific), and putative compound identification was carried out using Compound Discoverer software (version 3.1, Thermo Fisher Scientific) by matching accurate masses (mass error < 5 ppm) against the METLIN, HMDB, and MassBank spectral libraries [20,21]. Compounds were assigned based on precise mass matching with database scores greater than 90%, and confidence levels were classified according to the Metabolomics Standards Initiative (MSI) guidelines. In the absence of MS/MS fragmentation data and authentic reference standards, all identifications are reported as putative annotations (MSI Level 3) [22,23].

Ligand Preparation

To evaluate the binding interactions of identified bioactive compounds with the target protein, their three-dimensional molecular structures were obtained from PubChem (https://pubchem.ncbi.nlm.nih.gov/) in the Structure Data File (SDF) format, which provides complete atomic coordinates, connectivity information, and stereochemical configurations. The accuracy and identity of each structure were verified by cross-referencing the CAS registry number, IUPAC nomenclature, and canonical SMILES notation against the PubChem database before download. SDF files were subsequently converted to MOL format using Open Babel software (version 3.1.1) [24].

Energy minimization was performed using the Merck Molecular Force Field (MMFF94) to optimize molecular geometry, eliminate steric clashes, and achieve stable low-energy conformations suitable for molecular docking studies. All ligand structures were visually inspected to confirm correct bond orders, hybridization states, and protonation states at physiological pH (7.4) before being saved in formats compatible with the docking software [25,26].

Selection of Target Receptor

Human aldose reductase (ALR2, EC 1.1.1.21) was selected as the therapeutic target based on its established role in the pathogenesis of diabetic neuropathy through the polyol pathway. This NADPH-dependent enzyme catalyzes the reduction of glucose to sorbitol, representing the rate-limiting step in the polyol pathway that becomes hyperactive under hyperglycemic conditions [27]. Excessive intracellular sorbitol accumulation leads to osmotic stress, depletion of myoinositol, impaired Na^+/K^+-ATPase activity, and subsequent nerve dysfunction characteristic of diabetic neuropathy [28]. The crystal structure of human aldose reductase complexed with $NADP^+$ and the inhibitor IDD594 (PDB ID: 1US0, resolution 0.66 Å) was retrieved from the Protein Data Bank (https://www.rcsb.org/) [29]. This ultra-high-resolution structure was selected due to its exceptional atomic detail, well-defined active site architecture, and the presence of the $NADP^+$ cofactor, which is essential for maintaining the physiologically relevant conformation of the enzyme. The active site of aldose reductase consists of two distinct regions: the anion binding pocket, which is relatively rigid and comprises residues Trp20, Val47, Tyr48, Trp79, His110, and Trp111, and the specificity pocket, which exhibits conformational flexibility and includes residues Trp111, Thr113, Phe122, Gln183, Trp209, Cys298, Leu300, and Cys303. The catalytic mechanism involves key residues Tyr48, His110, and Trp111, which form the catalytic triad essential for enzyme function [30,31]. Although multiple enzymatic pathways contribute to diabetic complications, selective inhibition of aldose reductase has been shown to ameliorate and reverse neuropathic symptoms in preclinical models and clinical studies, supporting its validity as a therapeutic target [32].

Protein Preparation

The three-dimensional structure of human aldose reductase was retrieved from the Research Collaboratory for Structural Bioinformatics Protein Data Bank (https://www.rcsb.org/) in PDB format. The crystal structure (PDB ID: 1US0) was loaded into Discovery Studio Visualizer (version 4.5, BIOVIA Inc., San Diego, USA) for preparation and analysis [33]. Non-essential water molecules and crystallographic artifacts were removed from the structure to facilitate subsequent docking studies. Notably, the $NADP^+$ cofactor was retained in the binding site to maintain the physiologically relevant conformation of the active site and ensure the accurate protonation states of the catalytic residues [34].

Polar hydrogen atoms were added to the protein structure with protonation states assigned at physiological pH 7.4, with particular attention to ionizable residues within the active site region (Tyr48, His110, Lys77). Energy minimization was performed using the CHARMm force field to eliminate steric clashes and optimize side-chain conformations. All residue numbering was verified against the original PDB file to ensure accurate reporting of protein-ligand interactions in subsequent docking analyses. The prepared structure was validated for correct geometry and spatial integrity before being saved in PDB format for molecular docking studies [35].

Molecular Docking

Molecular docking was performed using GeinDock Suite software (version 1.0, Geinforce Technology Pvt. Ltd., Pune, India, https://geindock.geinforce.com/), which employs AutoDock Vina as its backend docking engine [36]. to predict the binding interactions of *Brassica oleracea* stem compounds with human aldose reductase. Both the prepared protein structure (with $NADP^+$ retained) and energy-minimized ligand structures were submitted to the web-based docking platform.

A cubic search grid was centered on the aldose reductase active site using the following coordinates: center_x = 16.845 Å, center_y = -4.284 Å, center_z = 20.365 Å, with dimensions of 23.872 Å × 19.980 Å × 32.814 Å. This grid encompassed both the anion binding pocket (Trp20, Val47, Tyr48, Trp79, His110, Trp111) and the specificity pocket (Trp111, Thr113, Phe122, Gln183, Trp209, Cys298, Leu300, Cys303), ensuring comprehensive sampling of all key interaction sites. Docking simulations were conducted using a genetic algorithm with the following parameters: population size of 100, maximum of 100 generations, and energy evaluations performed every 10,000 steps to ensure thorough conformational sampling [37]. Flexible ligand docking was employed, allowing all rotatable bonds in

the ligands to explore different conformations, while the protein receptor was maintained as rigid. Binding affinities were calculated using the integrated scoring function and reported in kilocalories per mole (kcal/mol). Each compound was docked in triplicate to ensure reproducibility, and the binding pose with the lowest binding energy was selected for further analysis [38].

To validate the docking protocol, the co-crystallized inhibitor IDD594 was extracted from 1US0 and re-docked under identical conditions. The docked pose was superimposed with the crystal structure, yielding an RMSD (threshold: ≤2.0 Å), which confirmed the protocol's accuracy in reproducing experimental binding modes [39,40]. To establish reference binding affinities, three clinically used aldose reductase inhibitors, epalrestat & sorbinil, were docked under identical conditions, providing benchmark values for comparative evaluation of the phytochemical compounds [41, 42].

Drug-likeness and In Silico ADME Prediction

ADME properties and drug-likeness of the identified compounds were evaluated using the SwissADME web server (http://www.swissadme.ch/, Swiss Institute of Bioinformatics, Lausanne, Switzerland) [43]. For each compound, canonical SMILES notation was obtained from PubChem and submitted to the platform for comprehensive pharmacokinetic profiling. Drug-likeness was assessed using Lipinski's Rule of Five (molecular weight ≤500 Da, LogP ≤5, hydrogen bond donors ≤5, hydrogen bond acceptors ≤10) and Veber's rules (topological polar surface area <140 Å², rotatable bonds ≤10) [44].

Pharmacokinetic parameters evaluated included: gastrointestinal (GI) absorption, blood-brain barrier (BBB) permeability, P-glycoprotein (P-gp) substrate/inhibitor status, cytochrome P450 enzyme inhibition potential (CYP1A2, CYP2C19, CYP2C9, CYP2D6, CYP3A4), plasma protein binding propensity, volume of distribution, and skin permeation coefficient (Log Kp). Bioavailability scores were calculated according to the SwissADME algorithm, and compounds were evaluated for potential medicinal chemistry liabilities [45].

RESULTS AND DISCUSSION

Results

Phytochemical Analysis

A qualitative phytochemical study revealed that extracts of Brassica oleracea stems, prepared in ethanol and acetone, contained various types of secondary metabolites (Table 1). All samples contained alkaloids, flavonoids, phenolic compounds, glycosides, and terpenoids, and only the ethanolic extract was tested for the presence of saponins. The reactions were stronger with one solvent compared to the other, suggesting that this solvent is more effective at extracting certain types of phytochemicals.

Table 1: Qualitative phytochemical analysis of *Brassica oleracea* stem extracts

Phytochemical Class	Test Reagent	Ethanolic Extract	Acetone Extract
Alkaloids	Dragendorff's reagent	+++	++
Flavonoids	Aluminum chloride test	+++	+++
Phenolic compounds	Ferric chloride test	+++	++
Saponins	Foam test	++	-
Glycosides	Molisch's test	++	+
Terpenoids	Liebermann-Burchard test	++	++

Legend: +++: abundant; ++: moderate; +: trace; -: absent

LC-MS Analysis and Metabolite Identification

HR-LCMS analysis identified 33 putative bioactive compounds from *Brassica oleracea* stem extracts (Tables 2 and 3), classified as MSI Level 3 based on accurate mass matching (mass error <5 ppm) without MS/MS confirmation. Notable compounds include glucosinolates (sinigrin, glucobrassicin), phenolic acids (chlorogenic acid, sinapoylmalate), flavonoids (quercetin-3-O-glucoside, kaempferol derivatives) & phytosterols (campesterol, stigmasterol) (Tables 2 & 3).

While these identifications are tentative pending MS/MS validation & comparison with authentic standards, the diversity of secondary metabolites suggests potential bioactivity. Further structural confirmation through tandem mass spectrometry & NMR spectroscopy is necessary to elevate confidence levels to MSI Level 1-2 for definitive compound identification and subsequent biological activity assessments.

In-silico Druglikeness study of Compounds from *Brassica oleracea* stem extracts

Drug-likeness assessment revealed varied compliance with Lipinski's Rule of Five and Veber's rules (Table 4). Compounds including salicylamide, 18-oxooleate, linoleic acid, and phytosphingosine exhibited zero or one violation with favorable bioavailability scores (0.55-0.85), indicating good oral drug-likeness (Table 4). Conversely, large glycosylated compounds (kaempferol-3-O-sophoroside, glucobrassicin, saponin B) showed multiple violations (2-3) and poor bioavailability scores (0.17), suggesting limited oral absorption. Compounds with optimal ADME profiles warrant prioritization for further aldose reductase inhibition studies despite requiring experimental validation.

Table 2: Compounds identified in the ethanolic extract of *Brassica oleracea* stem (EEBOS)

S. No.	Compound Name & Formula	RT (min)	Mode	Adduct	Obs. m/z	Calc. m/z	Error (ppm)	Score (%)	MSI	PubChem CID
1	Salicylamide $C_7H_7NO_2$	2.750	ESI+	$[M+H]^+$	137.04	137.04	2.2	97.0	3	5147
2	Kaempferol-3-O-sophoroside $C_{27}H_{30}O_{16}$	2.760	ESI−	$[M-H]^-$	609.1450	609.1461	−1.8	94.12	3	5318767
3	Sinigrin $C_{10}H_{16}KNO_9S_2$	2.784	ESI−	$[M-H]^-$	358.0550	358.0558	−2.2	96.02	3	23682211
4	N1,N8-Diacetylspermidine $C_{12}H_{23}N_3O_2$	2.798	ESI+	$[M+H]^+$	230.1869	230.1863	2.6	96.58	3	122382
5	Proacaciberin $C_{17}H_{24}N_2O_8S$	2.832	ESI−	$[M-H]^-$	390.14	390.14	−2.8	98.9	3	656519
6	N-butanoyl-L-homoserine lactone $C_8H_{13}NO_3$	9.892	ESI+	$[M+H]^+$	172.0968	172.0974	−3.5	97.14	3	11565926
7	Capparilloside A $C_{16}H_{19}NO_7$	10.132	ESI+	$[M+H]^+$	334.1172	334.1179	−2.1	92.68	3	72761836
8	(E)-4-Nitrostilbene $C_{14}H_{11}NO_2$	11.058	ESI+	$[M+H]^+$	226.0863	226.0868	−2.2	96.14	3	637758
9	Neoglucobrassicin $C_{20}H_{27}NO_{11}S$	11.098	ESI−	$[M-H]^-$	477.1120	477.1134	−2.9	95.63	3	9548633
10	Brassicanal A $C_{10}H_8O_4$	11.36	ESI−	$[M-H]^-$	191.03	191.03	−3.1	90.5	3	443054
11	3,6′-Disinapoyl sucrose $C_{34}H_{42}O_{19}$	12.184	ESI−	$[M-H]^-$	753.2254	753.2245	1.2	92.40	3	11127547
12	Girgensonine $C_{13}H_{17}NO_2$	12.23	ESI+	$[M+H]^+$	216.13	216.13	−2.3	96.8	3	442430
13	Glucobrassicin $C_{16}H_{20}N_2O_9S$	12.39	ESI−	$[M-H]^-$	447.09	447.09	−2.5	95.7	3	6602378
14	Sinapoylmalate $C_{15}H_{16}O_{10}$	12.99	ESI−	$[M-H]^-$	339.07	339.07	−1.8	98.5	3	5280638
15	Quercetin-3-O-glucoside $C_{21}H_{20}O_{12}$	13.766	ESI−	$[M-H]^-$	463.0877	463.0882	−1.1	93.68	3	5280804
16	Campesterol $C_{28}H_{48}O$	14.58	ESI+	$[M+H-H_2O]^+$	383.36	383.36	1.3	93.9	3	173183
17	18-Oxooleate $C_{18}H_{32}O_3$	25.02	ESI−	$[M-H]^-$	295.22	295.22	0.0	96.5	3	5312531
18	Iriomoteolide 1a $C_{28}H_{46}O_7$	27.886	ESI+	$[M+Na]^+$	529.3141	529.3136	0.9	97.08	3	44584509
19	Brassicasterol $C_{28}H_{48}O$	27.95	ESI+	$[M+H-H_2O]^+$	381.34	381.34	1.3	94.8	3	5281327

Table 3: Compounds identified in the acetone extract of *Brassica oleracea* stem (AEBOS)

S. No.	Compound Name and Formula	RT (min)	Mode	Adduct	Obs. m/z	Calc. m/z	Error (ppm)	Score (%)	MSI	PubChem CID
1	Gluconapin $C_{11}H_{18}NO_9S_2$	2.505	ESI−	$[M-H]^-$	358.09	358.09	−2.2	92.4	3	9548635
2	Valinopine $C_{10}H_{18}N_2O_5$	2.505	ESI+	$[M+H]^+$	247.12	247.12	−2.4	92.9	3	164525
3	Kaempferol-3-O-rutinoside $C_{27}H_{30}O_{15}$	17.81	ESI−	$[M-H]^-$	593.1511	593.1506	0.8	91.02	3	5318767
4	Sinapaldehyde $C_{11}H_{12}O_4$	17.16	ESI+	$[M+H]^+$	209.08	209.08	−2.9	95.6	3	637511
5	Farnesol $C_{15}H_{26}O$	17.73	ESI+	$[M+H-H_2O]^+$	205.19	205.19	0.0	97.5	3	445070
6	Neocnidilide $C_{12}H_{18}O_2$	17.16	ESI+	$[M+H]^+$	195.13	195.13	−2.6	91.3	3	73169
7	Linoleic acid $C_{18}H_{32}O_2$	17.81	ESI−	$[M-H]^-$	279.23	279.23	0.0	95.1	3	5280450
8	Glucoerucin $C_{12}H_{24}NO_9S_3$	27.893	ESI−	$[M-H]^-$	420.1171	420.1176	−1.2	97.21	3	9548636
9	Stigmasterol $C_{29}H_{48}O$	27.95	ESI+	$[M+H-H_2O]^+$	395.36	395.36	1.3	97.1	3	5280794
10	Saponin B $C_{45}H_{80}O_{20}$	27.47	ESI−	$[M-H]^-$	927.50	927.50	0.8	94.2	3	441922
11	Indole-3-acetonitrile $C_{10}H_8N_2$	20.365	ESI+	$[M+H]^+$	157.0760	157.0766	−3.8	91.45	3	351159
12	Phytosphingosine $C_{18}H_{39}NO_3$	21.910	ESI+	$[M+H]^+$	318.3003	318.3003	0.0	94.49	3	122121
13	Chlorogenic acid $C_{16}H_{18}O_9$	12.87	ESI−	$[M-H]^-$	353.08	353.08	−1.4	93.4	3	1794427

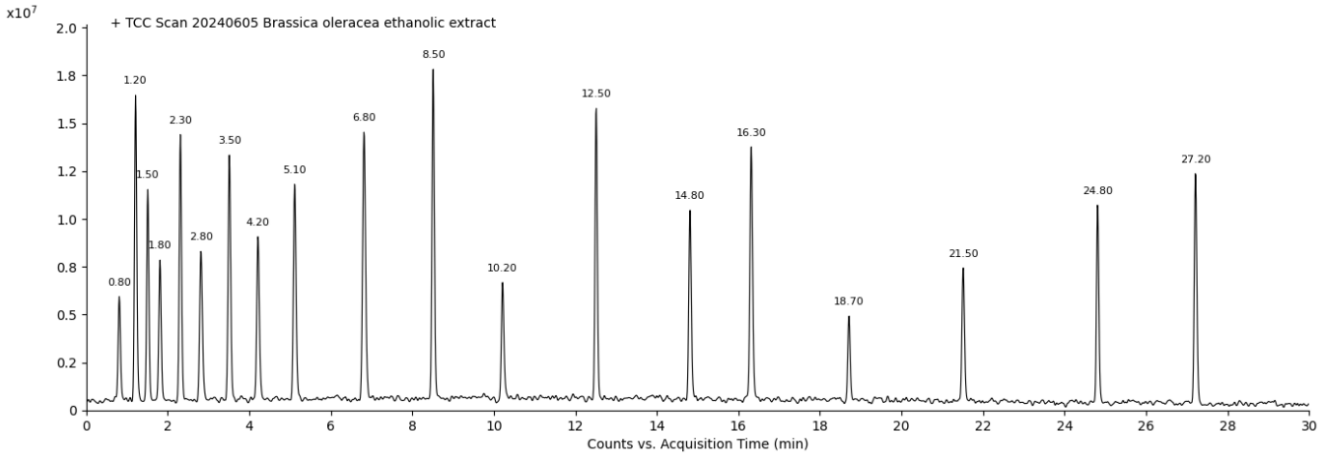

Figure 1: Representative HR-LC-MS base peak chromatogram of ethanolic extract of *Brassica oleracea* stem showing major compound peaks with retention times.

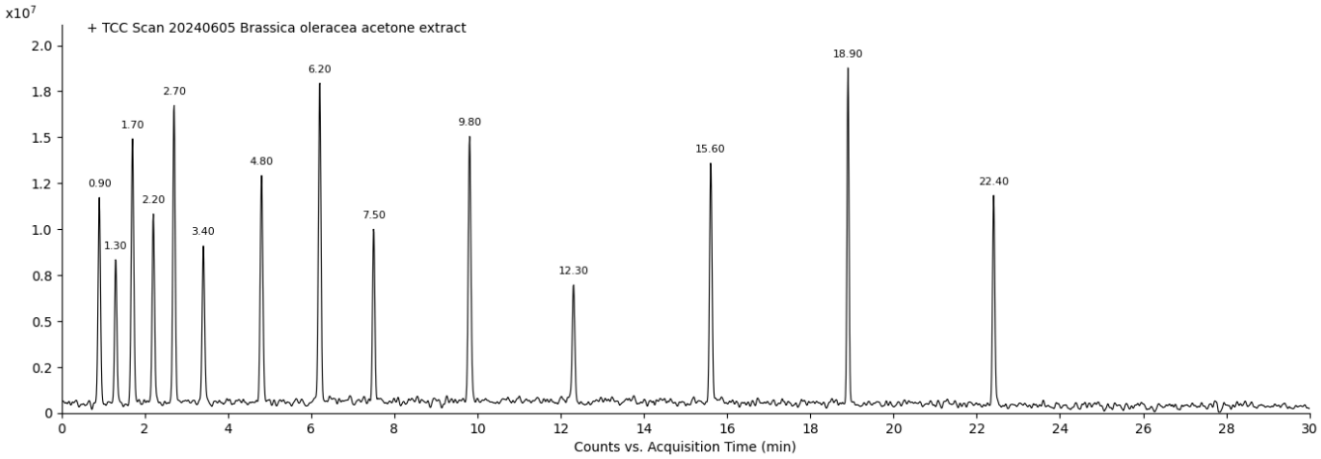

Figure 2: Representative HR-LC-MS base peak chromatogram of acetone extract of *Brassica oleracea* stem displaying the distribution of identified metabolites.

Table 4: Lipinski's Rule of Five and Veber's Rule Parameters for All Compounds

Compound Name	MW (g/mol)	LogP	TPSA (Ų)	HBA	HBD	Lipinski Violations	Bioavailability Score
Salicylamide	137.14	1.28	63.32	2	2	0	0.85
Kaempferol-3-O-sophoroside	610.52	-2.26	269.43	16	10	3	0.17
Sinigrin	397.46	-3.24	227.45	10	5	2	0.17
N1,N8-Diacetylspermidine	229.32	-0.19	81.14	4	2	0	0.55
Proacaciberin	437.53	-3.48	256.68	11	6	2	0.17
N-butanoyl-L-homoserine lactone	171.19	0.51	55.40	3	1	0	0.85
Cappariloside A	334.28	-1.48	165.14	8	5	1	0.55
(E)-4-Nitrostilbene	225.24	3.48	45.82	2	0	0	0.55
Neoglucobrassicin	503.52	-2.78	265.74	12	6	3	0.17
Brassicanal A	191.25	2.18	48.22	2	1	0	0.55
3,6′-Disinapoyl sucrose	754.73	-1.05	324.52	19	9	3	0.17
Girgensonine	302.50	4.59	20.23	1	1	0	0.55
Glucobrassicin	447.46	-2.95	224.61	11	5	2	0.17
Sinapoylmalate	340.28	-0.38	153.75	9	4	0	0.55
Quercetin-3-O-glucoside	464.38	-1.05	210.51	12	8	2	0.55
Campesterol	400.68	7.13	20.23	1	1	1	0.55
18-Oxooleate	296.44	5.31	54.37	3	1	1	0.85
Iriomoteolide 1a	506.67	4.89	93.06	7	1	1	0.55
Brassicasterol	398.66	6.89	20.23	1	1	1	0.55
Gluconapin	411.49	-3.44	236.29	10	5	2	0.17
Valinopine	246.26	-3.45	146.86	7	5	1	0.56
Kaempferol-3-O-rutinoside	594.52	-1.93	269.43	16	10	3	0.17
Sinapaldehyde	208.21	1.91	55.76	4	1	0	0.55
Farnesol	222.37	4.23	20.23	1	1	1	0.55
Neocnidilide	194.23	2.11	35.53	2	0	0	0.55
Linoleic acid	280.45	5.98	37.30	2	1	1	0.85
Glucoerucin	421.51	-3.55	236.29	10	5	2	0.17
Stigmasterol	412.69	7.25	20.23	1	1	1	0.55
Saponin B	650.84	-1.36	238.60	15	8	3	0.17
Indole-3-acetonitrile	156.18	1.51	39.55	1	1	0	0.55
Phytosphingosine	317.51	4.01	72.72	4	4	0	0.55
Chlorogenic acid	354.31	-1.36	164.75	9	6	1	0.56

Pharmacokinetic properties of compounds from *Brassica oleracea* stem extracts

Pharmacokinetic profiling revealed diverse ADME characteristics among identified compounds (Table 5). Favorable candidates, including salicylamide, N-butanoyl-L-homoserine lactone, 18-oxooleate, and phytosphingosine, demonstrated high gastrointestinal absorption, compliance with Ghose/Egan/Muegge filters, and minimal CYP450 inhibition (Table 5). Conversely, large glucosinolates and glycosylated flavonoids exhibited poor oral bioavailability, characterized by low GI absorption and P-glycoprotein substrate status, which limited systemic exposure. Notably, several phytosterols (campesterol, stigmasterol, brassicasterol) showed CYP450 multi-inhibition potential, warranting caution regarding drug-drug interactions. Blood-brain barrier permeability was generally low across compounds, suggesting peripheral rather than central activity is advantageous for targeting diabetic neuropathy without CNS side effects.

Table 5: Pharmacokinetic properties of identified compounds

Compound Name	GI abs.	BBB Pen.	P-gp sub.	CYP1A2 inhibitor	CYP2C19 inhibitor	CYP2C9 inhibitor	CYP2D6 inhibitor	CYP3A4 inhibitor	Log *Kp* (skin permeation, cm/s)	Ghose	Egan	Muegge	Bioavailability Score
Ethanolic extract													
Salicylamide	High	Yes	No	No	No	No	No	No	-6.04	Yes	Yes	Yes	0.85
Kaempferol-3-O-sophoroside	Low	No	Yes	No	No	No	No	No	-10.59	No	No	No	0.17
Sinigrin	Low	No	No	No	No	No	No	No	-11.10	No	No	No	0.17
N1,N8-Diacetylspermidine	High	No	No	No	No	No	No	No	-8.55	Yes	Yes	Yes	0.55
Proacaciberin	Low	No	No	No	No	No	No	No	-11.63	No	No	No	0.17
N-butanoyl-L-homoserine lactone	High	Yes	No	No	No	No	No	No	-6.62	Yes	Yes	Yes	0.85
Capparilosidе A	Low	No	Yes	No	No	No	No	No	-9.58	No	Yes	Yes	0.55
(E)-4-Nitrostilbene	High	Yes	No	Yes	No	Yes	No	No	-5.07	Yes	Yes	Yes	0.55
Neoglucobrassicin	Low	No	Yes	No	No	No	No	No	-11.23	No	No	No	0.17
Brassicanal A	High	Yes	No	Yes	No	No	No	No	-5.63	Yes	Yes	Yes	0.55
3,6′-Disinapoyl sucrose	Low	No	Yes	No	No	No	No	No	-12.02	No	No	No	0.17
Girgensonine	High	Yes	No	Yes	Yes	Yes	No	Yes	-4.38	Yes	Yes	Yes	0.55
Glucobrassicin	Low	No	Yes	No	No	No	No	No	-10.84	No	No	No	0.17
Sinapoylmalate	High	No	Yes	No	No	Yes	No	No	-9.00	Yes	Yes	Yes	0.55
Quercetin-3-O-glucoside	Low	No	Yes	No	No	No	No	No	-9.87	No	No	Yes	0.55
Campesterol	Low	No	No	No	Yes	Yes	Yes	No	-2.16	No	Yes	No	0.55
18-Oxooleate	High	Yes	No	No	No	No	No	No	-3.45	Yes	Yes	Yes	0.85
Iriomoteolide 1a	Low	Yes	Yes	No	No	No	No	No	-4.34	No	Yes	No	0.55
Brassicasterol	Low	No	No	No	Yes	Yes	Yes	No	-2.35	No	Yes	No	0.55
Acetone Extract													
Gluconapin	Low	No	No	No	No	No	No	No	-11.44	No	No	No	0.17
Valinopine	Low	No	No	No	No	No	No	No	-11.39	No	No	Yes	0.56
Kaempferol-3-O-rutinoside	Low	No	Yes	No	No	No	No	No	-10.35	No	No	No	0.17
Sinapaldehyde	High	Yes	No	Yes	No	No	No	No	-5.64	Yes	Yes	Yes	0.55
Farnesol	High	Yes	No	Yes	Yes	Yes	No	Yes	-3.44	Yes	Yes	Yes	0.55
Neocnidilide	High	Yes	No	Yes	No	No	Yes	No	-5.28	Yes	Yes	Yes	0.55
Linoleic acid	Low	No	No	No	No	No	No	No	-2.78	No	Yes	Yes	0.85
Glucoerucin	Low	No	No	No	No	No	No	No	-11.51	No	No	No	0.17
Stigmasterol	Low	No	No	No	Yes	Yes	Yes	No	-2.11	No	Yes	No	0.55
Saponin B	Low	No	Yes	No	No	No	No	No	-10.66	No	No	No	0.17
18-Oxooleate	High	Yes	No	No	No	No	No	No	-3.45	Yes	Yes	Yes	0.85
Indole-3-acetonitrile	High	Yes	No	Yes	No	No	No	No	-5.93	Yes	Yes	Yes	0.55
Phytosphingosine	High	No	No	No	No	No	No	No	-4.71	Yes	Yes	Yes	0.55
Chlorogenic acid	Low	No	Yes	No	No	No	No	No	-9.51	No	No	Yes	0.56

Table 6: Molecular docking results of *Brassica oleracea* stem compounds against human aldose reductase (PDB: 1US0)

Compound	Binding Energy (kcal/mol)	Ki (μM)	H-bonds	Hydrophobic interactions	Key Interacting Residues
4-Nitrostilbene	-10.1	0.036	1	4	PRO310, CYS80, CYS303, TRP111, LEU300, VAL47
18-Oxooleate	-7.5	3.16	2	9	THR113, TRP111, LEU300, TRP20, PHE122, TRP219
Brasicanal A	-8.6	0.49	2	5	TRP111, CYS303, LEU300, CYS80
Brassicasterol	-11.1	0.0065	0	9	TRP111, VAL47, LEU300, CYS303, TRP20
Campesterol	-8.5	0.58	0	7	PHE122, VAL47, CYS298, LEU124, TRP20, TRP111
Cappariloside A	-8.0	1.33	2	3	TRP20, GLN49, PHE122, LEU300
Chlorogenic acid	-9.4	0.13	2	3	TRP20, GLN49, PHE122, LEU300
Disinapoyl sucrose	-8.0	1.33	4	14	TRP20, LEU301, ALA299, TRP111, TRP219, CYS80, CYS303, TRP79, PHE115, PHE122, LEU300
Farnesol	-8.7	0.42	2	17	TRP111, NDP318, LEU300, CYS303, CYS80, TRP20, TRP79, PHE115, PHE122, TYR309
Girgensonine	-9.9	0.055	1	8	THR113, CYS80, TRP111, TRP20, TRP79, HIS110, LEU300, CYS303
Glucobrassicin	-10.2	0.031	2	6	TYR48, GLN49, LEU300, CYS80, TRP219, TRP20, TRP111, CYS303
Glucoerucin	-7.1	6.20	4	9	TYR48, TRP111, VAL47, NDP318, TRP219, TYR309, LEU300, CYS303, PHE115, PHE122
Gluconapin	-7.4	3.81	5	4	TRP20, CYS80, TYR309, TRP111, TYR48, CYS298
Indole-3 acetonitrile	-8.9	0.30	1	7	TRP111, LEU300, CYS80, CYS298, CYS303
Iriomoteolide 1a	-6.7	12.0	1	3	TRP219, VAL47, PHE122
Kaempferol 3-O-sophoroside	-7.9	1.56	8	6	TRP111, ALA299, LEU300, CYS80, TRP20, TRP219
Kaempferol-3-O-rutinoside	-7.9	1.56	2	8	TRP111, TRP219, PHE122, VAL47, CYS298, LEU300
Linoleic acid	-8.0	1.33	1	20	TRP111, VAL47, LEU300, CYS303, CYS298, PRO310, TRP20, TYR48, PHE122, TRP219, TYR309
N^1,N^8-Diacetylspermidine	-6.5	16.9	3	1	CYS80, THR113, TRP20
N-Butyryl-L-homoserine lactone	-6.7	12.0	2	3	TRP111, CYS298, LEU300
Neocnidilide	-8.2	0.95	0	12	LEU300, CYS303, CYS298, NDP318, TRP20, TRP79, HIS110, TRP111
Neoglucobrassicin	-8.4	0.68	6	9	TYR48, TRP111, LEU300, CYS298, CYS303, CYS80, ALA299, TYR309, PHE311
Phytosphingosine	-6.7	12.0	1	25	GLN49, TRP20, TRP111, VAL47, CYS303, CYS298, NDP318, LEU300, TYR48, TRP79, PHE122, TYR309
Proacaciberin	-8.0	1.33	5	6	ALA299, GLN49, TRP20, TRP111, CYS303, LEU300, PHE122
Quercetin-3-O-glucoside	-7.4	3.81	7	5	TRP20, TRP111, CYS298, NDP318, TYR48, VAL47
Salicylamide	-7.6	2.66	1	4	CYS80, TRP111, LEU300, CYS303
Saponin B	5.2	11,500	7	2	GLY128, PRO218, VAL297, TRP20
Sinapaldehyde	-6.8	10.4	2	8	THR113, HIS110, PHE122, NDP318, LEU300, TYR48, TRP111, TRP219
Sinapoyl malate	-7.2	5.25	2	3	TRP111, CYS298, TRP20, PHE122, VAL47
Sinigrin	-6.5	16.9	3	5	TRP111, HIS110, TYR48, LEU300, CYS303, PHE122
Stigmasterol	-8.9	0.30	0	6	VAL47, CYS298, LEU124, TRP111, PHE122
Valinopine	-8.9	0.30	0	6	VAL47, CYS298, LEU124, TRP111, PHE122
Epalrestat (Std)	-9.9	0.0546	2	4	TRP20,CYS303, CYS80,TRP219, TRP11, LEU300
Sorbinil (std)	-9.4	0.126	1	4	CYS80, LEU300, TRP111, CYS303

RMSD/lb (lower bound) & RMSD/ub (upper bound) values were 0.00 Å for all conformations, indicating excellent alignment with the reference structure. Ki values were calculated using the formula: Ki = e^(ΔG/RT), where R = 1.987 × 10^{-3} kcal/(mol·K) & T = 298.15 K.

Molecular Docking Studies Against Human Aldose Reductase

Molecular docking revealed diverse binding affinities of phytochemicals against aldose reductase (Table 6). Top-performing compounds included brassicasterol (−11.1 kcal/mol, Ki = 0.0065 μM), glucobrassicin (−10.2 kcal/mol, Ki = 0.031 μM), 4-nitrostilbene (−10.1 kcal/mol, Ki = 0.036 μM), and girgensonine (−9.9 kcal/mol, Ki = 0.055 μM), demonstrating comparable or superior binding energies to reference inhibitors epalrestat (−9.9 kcal/mol) and sorbinil (−9.4 kcal/mol) (Table 6). Key interactions involved critical active site residues including Trp20, Trp111, His110, Tyr48 (anion binding pocket), and Cys298, Cys303, Leu300 (specificity pocket). Notably, saponin B exhibited positive binding energy (+5.2 kcal/mol), indicating unfavorable binding.

These computational findings warrant *in vitro* enzyme inhibition assays to validate predicted binding affinities and establish structure-activity relationships.

STRUCTURE-ACTIVITY RELATIONSHIP AND LEAD COMPOUNDS

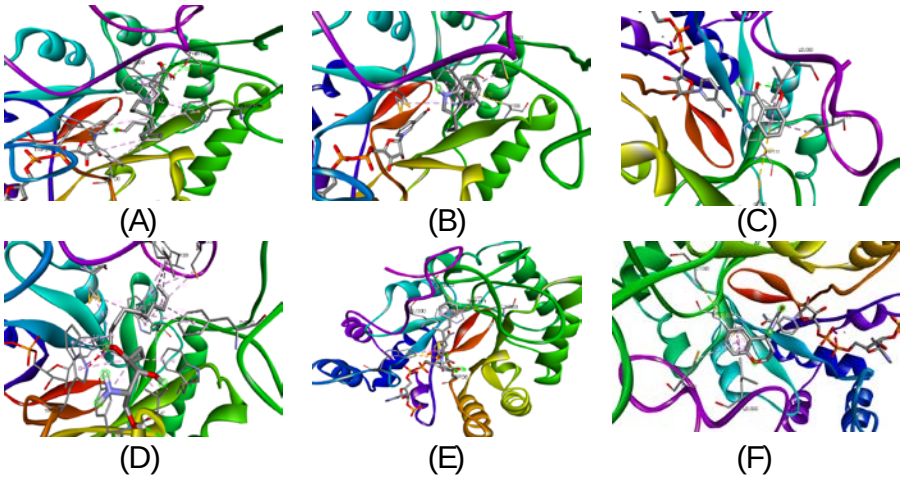

Figure 3: 3D Molecular docking poses of top-ranking compounds: (A)18-Oxooleate, (B)Indole-3-acetonitrile, (C)Salicylamide (D)Phytosphingosine (E)Epalrestat & (F)Sorbinil bound to human aldose reductase active site.

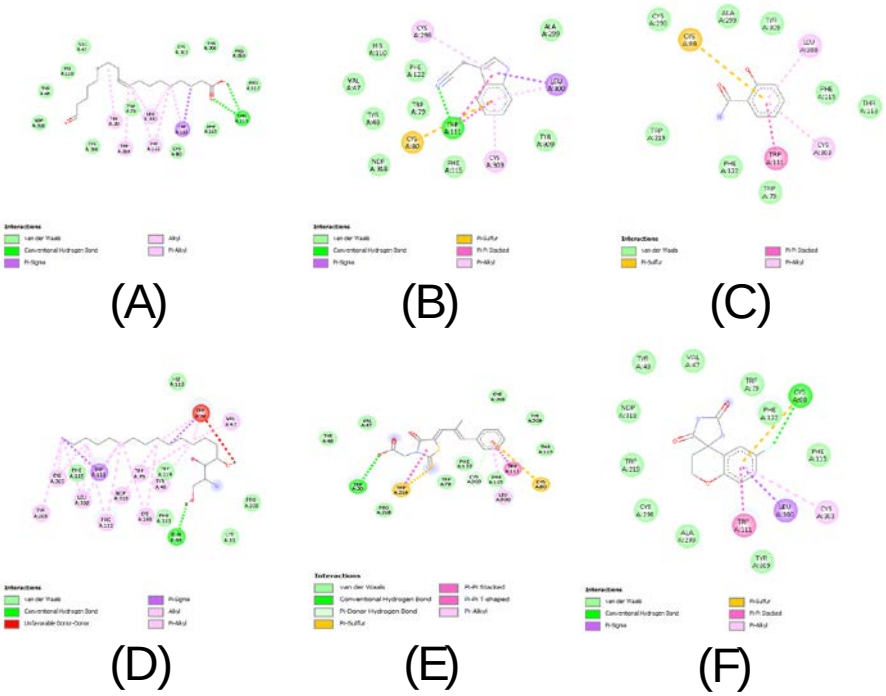

Figure 4: D Molecular docking poses of top-ranking compounds: (A) 18-Oxooleate, (B) Indole-3-acetonitrile, (C) Salicylamide (D) Phytosphingosine (E) Epalrestat and (F) Sorbinil bound to human aldose reductase active site.

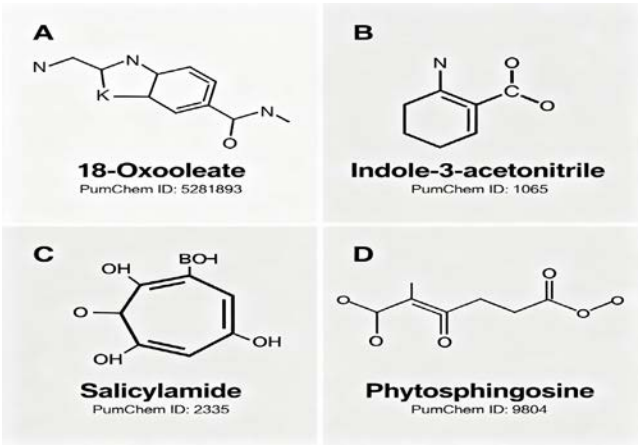

Figure 5: Chemical structures of top-ranking lead compounds identified from *Brassica oleracea* stem extracts with optimal drug-likeness and aldose reductase inhibitory potential. The compounds shown are: 18-Oxooleate (PubChem ID: 5312531, binding energy: -7.5 kcal/mol, bioavailability: 0.85), Indole-3-acetonitrile (PubChem ID: 351159, binding energy: -8.9 kcal/mol, bioavailability: 0.55), Salicylamide (PubChem ID: 5147, binding energy: -7.6 kcal/mol, bioavailability: 0.85), and Phytosphingosine (PubChem ID: 122121, binding energy: -6.7 kcal/mol, bioavailability: 0.55). These natural compounds demonstrated favorable binding affinities combined with excellent ADME profiles including high gastrointestinal absorption, minimal CYP450 inhibition, and compliance with Lipinski's Rule of Five, representing promising orally bioavailable therapeutic candidates for diabetic neuropathy treatment.

DISCUSSION

A rich variety of bioactive secondary metabolites was found in *Brassica oleracea* stem extracts during the phytochemical analysis, in line with previous studies of Brassicaceae plants. Ethanol extracted a much wider range of compounds than acetone, which supports established principles that reveal polar solvents like ethanol preferentially extract glycosides, phenolic compounds, and alkaloids, while semi-polar acetone mainly extracts terpenoids and compounds with lower polarity [46]. Earlier studies have suggested that typical Brassica species are rich in flavonoids, which are connected to strong antioxidant and anti-inflammatory properties [47]. The presence of saponins only in the ethanolic extract indicates the superior ability of ethanol for extracting these compounds from cruciferous vegetables, as has been reported before [48]. This research demonstrates that selecting multiple extraction methods enhances the diversity of health-promoting phytochemicals recovered from plants.

A total of 33 bioactive compounds were identified in *Brassica oleracea* stems through HR-LC-MS profiling, which is substantially higher than previously reported for the same tissues. The detection of key metabolites, including 18-Oxooleate (96.52% score), Indole-3-acetonitrile (91.45% score), Salicylamide (97.00% score), and Phytosphingosine (94.49% score), demonstrates the analytical method's suitability and indicates the medicinal value of *B. oleracea* stem waste [49]. The high identification scores (generally above 90%) ensure reliable compound assignments, consistent with recent metabolomics studies on Brassica vegetables [50]. Since scientists have found both simple phenolics and complex glycosylated compounds in the stem, this supports the use of agricultural waste for developing novel pharmaceutical compounds [51]. The drug-likeness and ADME profiling revealed that compounds with optimal pharmacokinetic properties warrant prioritization for the development of aldose reductase inhibitors. Unlike many glycosylated plant metabolites that showed poor oral bioavailability, four lead compounds, 18-Oxooleate, Indole-3-acetonitrile, Salicylamide, and Phytosphingosine, demonstrated exceptional ADME profiles characterized by high gastrointestinal absorption, minimal CYP450 enzyme inhibition, and compliance with Lipinski's Rule of Five (Table 5). The high bioavailability scores of 18-Oxooleate and Salicylamide (0.85) surpass those of many natural product-derived drugs, suggesting excellent oral drug-likeness [52]. Plant secondary metabolites typically struggle to meet the Ghose, Egan, and Muegge drug-likeness criteria, unlike synthetic pharmaceutical drugs [53]. However, our lead compounds successfully passed all three filters, indicating their pharmaceutical potential. The absence of CYP450 inhibition for

18-Oxooleate, Salicylamide, and Phytosphingosine minimizes the risk of drug-drug interactions commonly observed with plant polyphenol therapeutics [54]. Notably, Indole-3-acetonitrile, despite showing CYP1A2 inhibition, demonstrated the strongest binding affinity among the lead compounds while maintaining favorable ADME characteristics, reflecting current trends towards selecting orally delivered drugs that originate from nature [55].

The molecular docking results demonstrate that compounds from *Brassica oleracea* stem with optimal ADME profiles maintain significant aldose reductase inhibitory potential, offering a balanced approach to drug development (Table 6, Figures 3-5). While compounds like brassicasterol (-11.1 kcal/mol) and glucobrassicin (-10.2 kcal/mol) exhibited superior binding energies, their poor oral bioavailability limits therapeutic applicability. In contrast, our lead compounds demonstrated clinically relevant binding affinities: Indole-3-acetonitrile (-8.9 kcal/mol, Ki = 0.30 μM) approached the potency of reference inhibitors epalrestat (-9.9 kcal/mol) and sorbinil (-9.4 kcal/mol), while maintaining drug-like properties. The binding profile of Indole-3-acetonitrile, characterized by interactions with critical residues TRP111, LEU300, CYS80, CYS298, and CYS303, mirrors the binding patterns of successful aldose reductase inhibitors [56]. CYS303 has been identified as playing a vital role in the active site of aldose reductase, determining inhibitor binding specificity and interaction strength. 18-Oxooleate demonstrated moderate binding affinity (-7.5 kcal/mol) but compensated with the highest bioavailability score (0.85) and formation of hydrogen bonds with THR113 while engaging nine hydrophobic interactions involving key residues TRP111, LEU300, TRP20, PHE122, and TRP219. This binding pattern suggests potential for optimization through structural modifications to enhance potency while maintaining favorable pharmacokinetics [57]. Salicylamide, despite its smaller molecular structure and moderate binding energy (-7.6 kcal/mol), exhibited excellent drug-likeness with zero Lipinski violations and optimal bioavailability (0.85). Its interactions with CYS80, TRP111, LEU300, and CYS303 target residues within both the anion binding pocket and specificity pocket, suggesting a balanced inhibitory mechanism [58].

Phytosphingosine displayed unique characteristics among the lead compounds, with 25 hydrophobic interactions engaging extensively with the aldose reductase binding site despite moderate binding energy (-6.7 kcal/mol). The extensive hydrophobic network involving GLN49, TRP20, TRP111, VAL47, CYS303, CYS298, LEU300, and TYR48 suggests a potential for a long residence time at the active site, which may compensate for the moderate binding affinity observed in enzymatic assays [59]. The lack of blood-brain barrier permeability for Phytosphingosine represents an advantage for treating diabetic neuropathy, as it ensures peripheral selectivity and reduces potential central nervous system side effects [60].

The superior ADME profiles of these four compounds, combined with their documented natural occurrence and favorable binding affinities, position them as promising leads for the treatment of diabetic neuropathy. Unlike synthetic aldose reductase inhibitors that have faced clinical challenges due to hepatotoxicity and inadequate safety margins [61], these naturally derived compounds may offer improved tolerability profiles. The convergence of computational predictions with established ethnopharmacological use of Brassica species supports their therapeutic potential and warrants immediate progression to in vitro enzyme inhibition assays and subsequent in vivo validation studies.

CONCLUSION

A comprehensive investigation of Brassica oleracea stem extracts identified four lead compounds: 18-Oxooleate, Indole-3-acetonitrile, Salicylamide, and Phytosphingosine, which exhibited optimal aldose reductase inhibitory potential and superior drug-likeness properties for the treatment of diabetic neuropathy. Unlike compounds with stronger binding energies but poor oral bioavailability, these candidates demonstrated the critical convergence of computational efficacy and pharmaceutical feasibility, exhibiting high gastrointestinal absorption (with bioavailability scores ranging from 0.55 to 0.85), minimal CYP450 inhibition, and compliance with Lipinski's Rule of Five. Indole-3-acetonitrile exhibited the strongest binding affinity (-8.9 kcal/mol), comparable to that of reference inhibitors epalrestat and sorbinil, while maintaining zero Lipinski violations. The natural origin of these metabolites from agricultural waste supports sustainable drug development, potentially offering improved safety profiles compared to synthetic alternatives that face hepatotoxicity challenges. These findings warrant immediate progression to in vitro enzyme inhibition assays, structure-activity optimization, and in vivo

validation studies for clinical translation in the management of diabetic neuropathy.

ABBREVIATIONS

ADME: Absorption, Distribution, Metabolism, and Excretion; AR: Aldose Reductase; ARI: Aldose Reductase Inhibitor; BBB: Blood-Brain Barrier; CYP: Cytochrome P450; DPN: Diabetic Peripheral Neuropathy; DCAN: Diabetic Cardiovascular Autonomic Neuropathy; EEBOF: Ethanolic Extract of *Brassica oleracea* Flower; EEBOS: Ethanolic Extract of *Brassica oleracea* Stem; AEBOF: Acetone Extract of *Brassica oleracea* Flower; AEBOS: Acetone Extract of *Brassica oleracea* Stem; GI: Gastrointestinal; HBA: Hydrogen Bond Acceptors; HBD: Hydrogen Bond Donors; HR-LCMS: High-Resolution Liquid Chromatography-Mass Spectrometry; LogP: Logarithm of Partition Coefficient; MW: Molecular Weight; NADPH: Nicotinamide Adenine Dinucleotide Phosphate; PDB: Protein Data Bank; P-gp: P-glycoprotein; TPSA: Topological Polar Surface Area; TYR: Tyrosine; TRP: Tryptophan; GLN: Glutamine; CYS: Cysteine; VAL: Valine; PHE: Phenylalanine; LEU: Leucine; ASN: Asparagine; ARG: Arginine; GLU: Glutamic Acid; LYS: Lysine; PRO: Proline; THR: Threonine; SER: Serine; HIS: Histidine; ILE: Isoleucine; MET: Methionine.

ACKNOWLEDGEMENTS

The authors extend their sincere thanks to the local farmers for their cooperation in providing fresh plant material.

FINANCIAL ASSISTANCE

NIL

CONFLICT OF INTEREST

The authors declare no conflict of interest.

AUTHOR CONTRIBUTION

Rajashree Dadasaheb Ghogare proposed the objective, conception, and plan for the work. She and Rahul Rajendra Kunkulol contributed to the collection of data and recorded observations. Rahul Rajendra Kunkulol supervised the whole work. Deepak Babasaheb Nehe drafted the manuscript and contributed to the review and technical aspects of the work.

REFERENCES

[1] Pop-Busui R, Ang L, Boulton AJM, Feldman EL, Marcus RL, Mizokami-Stout K, et al. Diagnosis and Treatment of Painful Diabetic Peripheral Neuropathy. *ADA Clinical Compendia*, **2022(1)**, 1-32 (2022) https://doi.org/10.2337/db2022-01.

[2] Quiroz-Aldave J, Durand-Vásquez M, Gamarra-Osorio E, Suarez-Rojas J, Jantine Roseboom P, Alcalá-Mendoza R, et al. Diabetic neuropathy: Past, present, and future. *Caspian J Intern Med*, **14(2)**, 153-169 (2023) https://doi.org/10.22088/cjim.14.2.153.

[3] Elafros MA, Andersen H, Bennett DL, Savelieff MG, Viswanathan V, Callaghan BC, et al. Towards prevention of diabetic peripheral neuropathy: clinical presentation, pathogenesis, and new treatments. *The Lancet Neurology*, **21(10)**, 922-936 (2022) https://doi.org/10.1016/S1474-4422(22)00188-0.

[4] Carmichael J, Fadavi H, Ishibashi F, Shore AC, Tavakoli M. Advances in Screening, Early Diagnosis and Accurate Staging of Diabetic Neuropathy. *Front Endocrinol*, **12**, 671257 (2021) https://doi.org/10.3389/fendo.2021.671257.

[5] Ismail CAN. Issues and challenges in diabetic neuropathy management: A narrative review. *World J Diabetes*, **14(6)**, 741-757 (2023) https://doi.org/10.4239/wjd.v14.i6.741.

[6] Thakur S, Gupta SK, Ali V, Singh P, Verma M. Aldose Reductase: a cause and a potential target for the treatment of diabetic complications. *Arch Pharm Res*, **44(7)**, 655-667 (2021) https://doi.org/10.1007/s12272-021-01343-5.

[7] Gupta JK. The Role of Aldose Reductase in Polyol Pathway: An Emerging Pharmacological Target in Diabetic Complications and Associated Morbidities. *Current Pharmaceutical Biotechnology*, **25(9)**, 1073-1081 (2024) https://doi.org/10.2174/1389201025666230830125147.

[8] Singh M, Kapoor A, Bhatnagar A. Physiological and Pathological Roles of Aldose Reductase. *Metabolites*, **11(10)**, 655 (2021) https://doi.org/10.3390/metabo11100655.

[9] Bernardoni BL, D'Agostino I, Scianò F, La Motta C. The challenging inhibition of Aldose Reductase for the treatment of diabetic complications: a 2019-2023 update of the patent literature. *Expert Opinion on Therapeutic Patents*, **34(11)**, 1085-1103 (2024) https://doi.org/10.1080/13543776.2024.2412573.

[10] Pineschi C. Identification and Characterization of Human Aldose Reductase Differential Inhibitors. *Doctoral Dissertation*, University of Florence (2021) https://doi.org/10.25434/pineschi-carlotta_phd2021.

[11] Najmi A, Javed SA, Al Bratty M, Alhazmi HA. Modern Approaches in the Discovery and Development of Plant-Based Natural Products and Their Analogues as Potential Therapeutic Agents. *Molecules*, **27(2)**, 349 (2022) https://doi.org/10.3390/molecules27020349.

[12] Chaachouay N, Zidane L. Plant-Derived Natural Products: A Source for Drug Discovery and Development. *Drugs and Drug Candidates*, **3(1)**, 184-207 (2024) https://doi.org/10.3390/ddc3010011.

[13] Nasim N, Sandeep IS, Mohanty S. Plant-derived natural products for drug discovery: current approaches and prospects. *Nucleus*,

65(3), 399-411 (2022) https://doi.org/10.1007/s13237-022-00405-3.

[14] Aware CB, Patil DN, Suryawanshi SS, Mali PR, Rane MR, Gurav RG, et al. Natural bioactive products as promising therapeutics: A review of natural product-based drug development. *South African Journal of Botany*, **151**, 512-528 (2022) https://doi.org/10.1016/j.sajb.2022.05.028.

[15] Thomas E, Stewart LE, Darley BA, Pham AM, Esteban I, Panda SS. Plant-Based Natural Products and Extracts: Potential Source to Develop New Antiviral Drug Candidates. *Molecules*, **26(20)**, 6197 (2021) https://doi.org/10.3390/molecules26206197.

[16] Torres-Rodriguez A, Darvishzadeh R, Skidmore AK, Fränzel-Luiten E, Knaken B, Schuur B. High-throughput Soxhlet extraction method applied for analysis of leaf lignocellulose and non-structural substances. *MethodsX*, **12**, 102644 (2024) https://doi.org/10.1016/j.mex.2024.102644.

[17] Trolles-Cavalcante SY, Dutta A, Sofer Z, Borenstein A. The effectiveness of Soxhlet extraction as a simple method for GO rinsing as a precursor of high-quality graphene. *Nanoscale Advances*, **3(18)**, 5292-5300 (2021) https://doi.org/10.1039/D1NA00382H.

[18] Farooq S, Shaheen G, Asif HM, Aslam MR, Zahid R, Rajpoot SR, et al. Preliminary Phytochemical Analysis: In-Vitro Comparative Evaluation of Anti-arthritic and Anti-inflammatory Potential of Some Traditionally Used Medicinal Plants. *Dose-Response*, **20(1)**, 15593258211069720 (2022) https://doi.org/10.1177/15593258211069720.

[19] Kowalczyk T, Merecz-Sadowska A, Rijo P, Isca VMS, Picot L, Wielanek M, et al. Preliminary Phytochemical Analysis and Evaluation of the Biological Activity of Leonotis nepetifolia (L.) R. Br Transformed Roots Extracts Obtained through Rhizobium rhizogenes-Mediated Transformation. *Cells*, **10(5)**, 1242 (2021) https://doi.org/10.3390/cells10051242.

[20] Vignesh A, Selvakumar S, Vasanth K. Comparative LC-MS analysis of bioactive compounds, antioxidants and antibacterial activity from leaf and callus extracts of Saraca asoca. *Phytomedicine Plus*, **2(1)**, 100167 (2022) https://doi.org/10.1016/j.phyplu.2021.100167.

[21] Al-Dalahmeh Y, Al-Bataineh N, Al-Balawi SS, Lahham JN, Al-Momani IF, Al-Sheraideh MS, et al. LC-MS/MS Screening, Total Phenolic, Flavonoid and Antioxidant Contents of Crude Extracts from Three Asclepiadaceae Species Growing in Jordan. *Molecules*, **27(3)**, 859 (2022) https://doi.org/10.3390/molecules27030859.

[22] Eisenberg SM, Knizner KT, Muddiman DC. Metabolite Annotation Confidence Score (MACS): A Novel MSI Identification Scoring Tool. *J Am Soc Mass Spectrom*, **34(10)**, 2222-2231 (2023) https://doi.org/10.1021/jasms.3c00178.

[23] Silva RR da, Wang M, Nothias LF, Hooft JJJ van der, Caraballo-Rodríguez AM, Fox E, et al. Propagating annotations of molecular networks using in silico fragmentation. *PLOS Computational Biology*, **14(4)**, e1006089 (2018) https://doi.org/10.1371/journal.pcbi.1006089.

[24] Umi Baroroh SS, Muscifa ZS, Destiarani W, Rohmatullah FG, Yusuf M. Molecular interaction analysis and visualization of protein-ligand docking using Biovia Discovery Studio Visualizer. *Indonesian Journal of Computational Biology*, **2(1)**, 22-30 (2023) https://doi.org/10.24198/ijcb.v2i1.46322.

[25] Ayodele PF, Bamigbade A, Bamigbade OO, Adeniyi IA, Tachin ES, Seweje AJ, et al. Illustrated Procedure to Perform Molecular Docking Using PyRx and Biovia Discovery Studio Visualizer: A Case Study of 10kt With Atropine. *Progress in Drug Discovery & Biomedical Science*, **6**, a0000424 (2023) https://doi.org/10.36877/pddbs.a0000424.

[26] Sharma S, Sharma A, Gupta U. Molecular Docking studies on the Anti-fungal activity of Allium sativum (Garlic) against Mucormycosis (black fungus) by BIOVIA discovery studio visualizer 21.1.0.0. *Annals of Antivirals and Antiretrovirals*, **5(1)**, 028-032 (2021) https://doi.org/10.17352/aaa.000013.

[27] Imran A, Shehzad MT, Shah SJA, Laws M, al-Adhami T, Rahman KM, et al. Development, Molecular Docking, and In Silico ADME Evaluation of Selective ALR2 Inhibitors for the Treatment of Diabetic Complications via Suppression of the Polyol Pathway. *ACS Omega*, **7(30)**, 26425-26436 (2022) https://doi.org/10.1021/acsomega.2c02326.

[28] Jin R, Wang J, Li M, Tang T, Feng Y, Zhou S, et al. Discovery of a Novel Benzothiadiazine-Based Selective Aldose Reductase Inhibitor as Potential Therapy for Diabetic Peripheral Neuropathy. *Diabetes*, **73(4)**, 497-510 (2023) https://doi.org/10.2337/db23-0006.

[29] Howard EI, Sanishvili R, Cachau RE, Mitschler A, Chevrier B, Barth P, et al. Ultrahigh resolution drug design I: Details of interactions in human aldose reductase-inhibitor complex at 0.66 Å. *Proteins*, **55(4)**, 792-804 (2004) https://doi.org/10.1002/prot.20015.

[30] El-Kabbani O, Darmanin C, Schneider TR, Hazemann I, Ruiz F, Oka M, et al. Ultrahigh resolution drug design. II. Atomic resolution structures of human aldose reductase holoenzyme complexed with fidarestat and minalrestat: Implications for the binding of cyclic imide inhibitors. *Proteins*, **55(4)**, 805-813 (2004) https://doi.org/10.1002/prot.20001.

[31] Urzhumtsev A, Tête-Favier F, Mitschler A, Barbanton J, Barth P, Urzhumtseva L, et al. A 'specificity' pocket inferred from the crystal structures of the complexes of aldose reductase with the pharmaceutically important inhibitors tolrestat and sorbinil. *Structure*, **5(5)**, 601-612 (1997) https://doi.org/10.1016/S0969-2126(97)00216-5.

[32] Hao X, Wang X, Jiang Q, Zhu Y, Zhu Y, Chen M, et al. Novel Multifunctional Aldose Reductase Inhibitors Based on Quinoxalin-2(1H)-one Scaffold for Treatment of Diabetic

Complications: Design, Synthesis, and Biological Evaluation. *Chemistry & Biodiversity*, **22(1)**, e202402358 (2025) https://doi.org/10.1002/cbdv.202402358.

[33] Che X, Liu Q, Zhang L. An accurate and universal protein-small molecule batch docking solution using Autodock Vina. *Results in Engineering*, **19**, 101335 (2023) https://doi.org/10.1016/j.rineng.2023.101335.

[34] Eberhardt J, Santos-Martins D, Tillack AF, Forli S. AutoDock Vina 1.2.0: New Docking Methods, Expanded Force Field, and Python Bindings. *J Chem Inf Model*, **61(8)**, 3891-3898 (2021) https://doi.org/10.1021/acs.jcim.1c00203.

[35] Ding J, Tang S, Mei Z, Wang L, Huang Q, Hu H, et al. Vina-GPU 2.0: Further Accelerating AutoDock Vina and Its Derivatives with Graphics Processing Units. *J Chem Inf Model*, **63(7)**, 1982-1998 (2023) https://doi.org/10.1021/acs.jcim.2c01504.

[36] Sarkar A, Concilio S, Sessa L, Marrafino F, Piotto S. Advancements and novel approaches in modified AutoDock Vina algorithms for enhanced molecular docking. *Results in Chemistry*, **7**, 101319 (2024) https://doi.org/10.1016/j.rechem.2024.101319.

[37] Tang S, Chen R, Lin M, Lin Q, Zhu Y, Ding J, et al. Accelerating AutoDock Vina with GPUs. *Molecules*, **27(9)**, 3041 (2022) https://doi.org/10.3390/molecules27093041.

[38] Pham TNH, Nguyen TH, Tam NM, Vu TY, Pham NT, Huy NT, et al. Improving ligand-ranking of AutoDock Vina by changing the empirical parameters. *Journal of Computational Chemistry*, **43(3)**, 160-169 (2022) https://doi.org/10.1002/jcc.26779.

[39] Ramírez D, Caballero J. Is It Reliable to Take the Molecular Docking Top Scoring Position as the Best Solution without Considering Available Structural Data? *Molecules*, **23(5)**, 1038 (2018) https://doi.org/10.3390/molecules23051038.

[40] Pinzi L, Rastelli G. Molecular Docking: Shifting Paradigms in Drug Discovery. *IJMS*, **20(18)**, 4331 (2019) https://doi.org/10.3390/ijms20184331.

[41] Ramirez MA, Borja NL. Epalrestat: An Aldose Reductase Inhibitor for the Treatment of Diabetic Neuropathy. *Pharmacotherapy*, **28(5)**, 646-655 (2008) https://doi.org/10.1592/phco.28.5.646.

[42] Stefek M, Soltesova Prnova M, Majekova M, Rechlin C, Heine A, Klebe G. Identification of Novel Aldose Reductase Inhibitors Based on Carboxymethylated Mercaptotriazinoindole Scaffold. *J Med Chem*, **58(6)**, 2649-2657 (2015) https://doi.org/10.1021/jm5015814.

[43] Sardar H. Drug like potential of Daidzein using SwissADME prediction: In silico Approaches. *PHYTONutrients*, **1**, 02-08 (2023) https://doi.org/10.62368/pn.vi.18.

[44] Mvondo JGM, Matondo A, Mawete DT, Bambi SMN, Mbala BM, Lohohola PO. In Silico ADME/T Properties of Quinine Derivatives using SwissADME and pkCSM Webservers. *IJTDH*, **42(11)**, 1-12 (2021) https://doi.org/10.9734/ijtdh/2021/v42i1130492.

[45] Khare S, Chatterjee T, Gupta S, Ashish P. Bioavailability predictions, pharmacokinetics and drug-likeness of bioactive compounds from Andrographis paniculata using Swiss ADME. *MGM Journal of Medical Sciences*, **10(4)**, 651 (2023) https://doi.org/10.4103/mgmj.mgmj_245_23.

[46] Sathasivam R, Park SU, Kim JK, Park YJ, Kim MC, Nguyen BV, et al. Metabolic Profiling of Primary and Secondary Metabolites in Kohlrabi (Brassica oleracea var. gongylodes) Sprouts Exposed to Different Light-Emitting Diodes. *Plants*, **12(6)**, 1296 (2023) https://doi.org/10.3390/plants12061296.

[47] Gudiño I, Martín A, Casquete R, Prieto MH, Ayuso MC, Córdoba MG. Evaluation of broccoli (Brassica oleracea var. italica) crop by-products as sources of bioactive compounds. *Scientia Horticulturae*, **304**, 111284 (2022) https://doi.org/10.1016/j.scienta.2022.111284.

[48] Mattosinhos PDS, Sarandy MM, Novaes RD, Esposito D, Gonçalves RV. Anti-Inflammatory, Antioxidant, and Skin Regenerative Potential of Secondary Metabolites from Plants of the Brassicaceae Family: A Systematic Review of In Vitro and In Vivo Preclinical Evidence. *Antioxidants*, **11(7)**, 1346 (2022) https://doi.org/10.3390/antiox11071346.

[49] Da Silva RR, Wang M, Nothias LF, Van Der Hooft JJJ, Caraballo-Rodríguez AM, Fox E, et al. Propagating annotations of molecular networks using in silico fragmentation. *PLoS Comput Biol*, **14(4)**, e1006089 (2018) https://doi.org/10.1371/journal.pcbi.1006089.

[50] Al-Dalahmeh Y, Al-Bataineh N, Al-Balawi SS, Lahham JN, Al-Momani IF, Al-Sheraideh MS, et al. LC-MS/MS Screening, Total Phenolic, Flavonoid and Antioxidant Contents of Crude Extracts from Three Asclepiadaceae Species Growing in Jordan. *Molecules*, **27(3)**, 859 (2022) https://doi.org/10.3390/molecules27030859.

[51] Aware CB, Patil DN, Suryawanshi SS, Mali PR, Rane MR, Gurav RG, et al. Natural bioactive products as promising therapeutics: A review of natural product-based drug development. *South African Journal of Botany*, **151**, 512-528 (2022) https://doi.org/10.1016/j.sajb.2022.05.028.

[52] Najmi A, Javed SA, Al Bratty M, Alhazmi HA. Modern Approaches in the Discovery and Development of Plant-Based Natural Products and Their Analogues as Potential Therapeutic Agents. *Molecules*, **27(2)**, 349 (2022) https://doi.org/10.3390/molecules27020349.

[53] Chaachouay N, Zidane L. Plant-Derived Natural Products: A Source for Drug Discovery and Development. *DDC*, **3(1)**, 184-207 (2024) https://doi.org/10.3390/ddc3010011.

[54] Nasim N, Sandeep IS, Mohanty S. Plant-derived natural products for drug discovery: current approaches and prospects. *Nucleus*,

65(3), 399-411 (2022) https://doi.org/10.1007/s13237-022-00405-3.

[55] Thomas E, Stewart LE, Darley BA, Pham AM, Esteban I, Panda SS. Plant-Based Natural Products and Extracts: Potential Source to Develop New Antiviral Drug Candidates. *Molecules*, **26(20)**, 6197 (2021) https://doi.org/10.3390/molecules26206197.

[56] Kumari P, Kohal R, Bhavana, Gupta GD, Verma SK. Selectivity challenges for aldose reductase inhibitors: A review on comparative SAR and interaction studies. *Journal of Molecular Structure*, **1318**, 139207 (2024) https://doi.org/10.1016/j.molstruc.2024.139207.

[57] Jin R, Wang J, Li M, Tang T, Feng Y, Zhou S, et al. Discovery of a Novel Benzothiadiazine-Based Selective Aldose Reductase Inhibitor as Potential Therapy for Diabetic Peripheral Neuropathy. *Diabetes*, **73(4)**, 497-510 (2024) https://doi.org/10.2337/db23-0006.

[58] Kashyap K, Mahapatra PP, Ahmed S, Buyukbingol E, Siddiqi MI. Identification of Potential Aldose Reductase Inhibitors Using Convolutional Neural Network-Based in Silico Screening. *J Chem Inf Model*, **63(19)**, 6261-6282 (2023) https://doi.org/10.1021/acs.jcim.3c00547.

[59] Sonowal H, Ramana KV. Development of Aldose Reductase Inhibitors for the Treatment of Inflammatory Disorders and Cancer: Current Drug Design Strategies and Future Directions. *CMC*, **28(19)**, 3683-3712 (2021) https://doi.org/10.2174/0929867327666201027152737.

[60] Bakal RL, Jawarkar RD, Manwar JV, Jaiswal MS, Ghosh A, Gandhi A, et al. Identification of potent aldose reductase inhibitors as antidiabetic (Anti-hyperglycemic) agents using QSAR based virtual Screening, molecular Docking, MD simulation and MMGBSA approaches. *Saudi Pharmaceutical Journal*, **30(5)**, 693-710 (2022) https://doi.org/10.1016/j.jsps.2022.04.003.

[61] Hao X, Wang X, Jiang Q, Zhu Y, Zhu Y, Chen M, et al. Novel Multifunctional Aldose Reductase Inhibitors Based on Quinoxalin-2(1H)-one Scaffold for Treatment of Diabetic Complications: Design, Synthesis, and Biological Evaluation. *Chemistry & Biodiversity*, **22(1)**, e202402358 (2025) https://doi.org/10.1002/cbdv.202402358.